Design and analysis of optical Y-splitters based on two-dimensional photonic crystal ring resonator

R. ARUNKUMAR[a,*], JAYSON K. JAYABARATHAN[b], S. ROBINSON[c]
[a,c]*Department of Electronics and Communication Engineering, Mount Zion College of Engineering and Technology, Pudukkottai, Tamil Nadu-622507, India*
[b]*Department of Computer Science Engineering, Mount Zion College of Engineering and Technology, Pudukkottai, Tamil Nadu-622507, India*

The power splitters are widely used in optical communication systems which are employed to distribute the input power into the output ports equally without any radiation or reflection losses. The proposed two-dimensional photonic crystal based power splitters are designed on a square lattice of circular silicon rods. In this work, 1×2, 1×3, 1×4 and 1×6 power splitters are proposed and designed. Except 1×2 splitter, the other three structures have a common diamond shaped structure of rods at the junction of the splitting region. The PBG of the devices are analyzed by the Plane Wave Expansion (PWE) method and their performance characteristics such as wavelength and transmission efficiency are evaluated using the Finite Difference Time Domain (FDTD) method. All the four designs show good performance and are able to provide considerable results.

(Received December 24, 2018; accepted August 20, 2019)

Keywords: Photonic crystal (PCs), Power splitter, Plane wave expansion (PWE), Finite difference time domain (FDTD)

1. Introduction

Photonic Crystals (PCs) are dielectric structures with periodic spatial alternations of the refractive index on the scale of wavelength of the light [1]. In general, PCs are composed of periodic dielectric, metallo-dielectric nanostructures which have alternative lower and higher dielectric constant materials in one, two and/or three dimensions to affect the propagation of electromagnetic waves inside the structure. As a result of this periodicity, the transmission of light is absolutely zero in certain frequency ranges which is called as Photonic Band Gap (PBG). By introducing defects in these periodic structures, the periodicity and thus the completeness of the PBG are entirely broken which allows to control and manipulate the light [2]. It ensures the localization of light in the PBG region which leads to the design of the PC based optical devices such as optical filters [3], multiplexers [4], de-multiplexers [5], directional couplers [6], power dividers/splitters [7], logic gates [8], switches [9], sensors [10], etc.

Typically, power splitters split the input power from one port to two or more output ports by a certain percentage with reduced losses. The key specifications of PC based power splitter design are to achieve low losses, good efficiency, wider bandwidth and compact size. At present time, the power splitters are being used in a wide range of communication applications.

Considering the specifications of a waveguide, a power splitter was designed by varying the combinations of the structure and was able to achieved about 80% efficiency [11]. A 3dB power splitter with a 180^o phase shift between the output signals was designed to split the incoming input signal [12]. The 1×4 power splitter made of 90^o sharp bends and T-branches was implemented on a square lattice of cylindrical rods [13]. A Photonic Crystal Waveguide (PCW) based 120^o Y-splitter was designed with and without the middle hole at an operating wavelength of 1310nm and the results showed that the efficiency was larger as much as 85% with the middle hole [14].

A 1×2 power splitter was designed with a hexagonal structure and was observed a transmission efficiency of 47.6% [15]. A MMI effect, a 1×2 splitter was proposed to operate at 1.55μm and achieved over 90% efficiency [16]. A rat-race circuit based 1×2 splitter/2×1 combiner was designed on a triangular lattice of dielectric rods in air [17]. A four-port 3dB splitter/combiner was proposed based on the coupled-mode theory [18]. The directional coupling based power splitter was designed and found to have a transmission of 96% with low-loss bends [19]. A hexagonal lattice PC based power splitter was analyzed based on the mode-splitting mechanism in the desired frequency range [20].

An ultracompact 3dB power splitter was designed based on triple PCW directional coupler with high transmission and wide bandwidth [21]. Unistructure and heterostructure based Y-splitters were investigated where the heterostructure splitter showed higher efficiency as much as 94% and two 1×4 power splitters were designed based on an optimized T-branch and two optimized 90^o bends which achieved equal splitting ratios at a wider bandwidth [22]. Photonic Crystal Ring Resonator (PCRR) based T-shaped power splitter was designed for a large bandwidth and showed high transmission efficiency of 98% [23]. The 1×2 and 1×4 power splitters were designed

based on waveguide directional coupling and resulted in a total transmission of about 96% and 92%, respectively [24]. The two-dimensional PC power dividers based on ring resonators and directional coupling were proposed and achieved 99% transmission [25].

A PC power splitter was designed by placing super defects at the junction of waveguides and was investigated to have 91% transmission with approximately equal power over both ports [26]. A bi-periodic Y-splitter was designed by choosing optimized values for period and radius of the rods and showed higher bandwidth and good transmission efficiency [27]. The hole-type PC structure based power splitter was designed on a triangular lattice where the defects were optimized by mode-splitting and position-shifting and achieved a transmission of over 45% per each output with a wider bandwidth [28]. The theoretical analysis of waveguide splitters showed that perfect transmission and zero reflection were attained under rate-matching, phase-matching and frequency-resonant conditions [29]. The power splitters based on PCW directional coupling were simulated with different power levels and achieved high transmission in a wider bandwidth [30].

An ultra-compact 2×2 power splitter was designed based on the asymmetric interference in MMI-based PCWs [31]. In a triangular PCW lattice of air holes, a new type of 3dB optical power splitter was proposed by utilizing PBGs [32]. The Y-junction power splitter was optimized by coupled mode theory which was able to control the output energy in the terahertz frequency range [33]. A 1×2 power splitter was designed on a PC slab made of Silicon-On-Insulator (SOI) material that showed high performance with ultra-low loss [34]. The results of the proposed 1×3 power splitter operated at three different wavelengths showed that the power was distributed almost equally with a total transmission of about 99.74% [35]. An optical power splitter was designed with three waveguides and two ring resonators which achieved 100% transmission [36]. The tunable dual-wavelength terahertz wave power splitter was operated on the basis of MMI effect and self-imaging principle [37]. By cascading asymmetric and symmetric 1×2 power splitters, a 1×3 splitter was designed with structural defects which achieved high output transmission and equal power distribution [38].

The 1×3 optical power splitter was designed and achieved a transmission of above 99% with a bandwidth of about 43nm [39]. A 1×3 power splitter was designed with dual ring resonators based on diamond inner rod configuration that showed equal power splitting at 1876nm [40]. On a triangular lattice of air holes, a new type of 1×4 splitter was implemented with one input PCW and two PC branches which obtained a total transmittance as high as 99.4% at 1550nm [41]. The eight channel power splitter was proposed based on 1×2 PCW and PC resonator that provided an equivalent power of 93.6% in the terahertz range [42]. Based on the similarities of cavity and whispering-gallery-like modes, 1×2 and 1×4 T-junction power dividers were designed [43].

Though there are several attempts are made with a different structure and different mechanism, the output from efficiency is tower and size is large. In this present work, PhC based power splitter has been designed and simulated for size namely 1x2, 1x3, 1x4, 1x6 structure and the effect of power splitter parameters also investigated. The remaining part of the paper, In section 2 represents the design of PhC based power splitter in different structural ranges of the proposed design. The field distribution of proposed power splitter and its significance are presented in section 3. In section 4 concludes the paper.

2. Structural design

Fig.1. shows the initial structure of the proposed design which is formed to design the V-shaped power splitter with 2D PCs square lattice with 21 ×21 rods. In the square lattice based design can modify the photonic band gap of the structure and achieve the required band gap as according to our requirements. In Silicon rods, the 'n' refractive index equals to 3.46 and rods have radii of r/a=0.1μm, where a=540nm.The band diagram in Fig. 2. gives the propagation modes of the structure without defect whose corresponding Brillouin zone is shown in Fig. 3

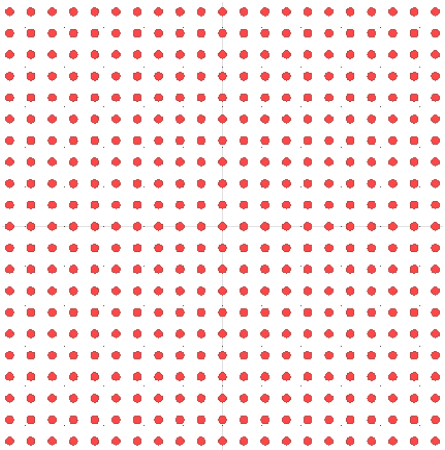

Fig. 1. Schematic structure of 21×21 photonic crystal structure

The Brillouin zone is the smallest repeating space in the periodic structure and hence the band diagram of single zone is equal to the whole zone. The band diagram is analyzed using the Plane Wave Expansion (PWE) method. In Fig. 2 (a), the "Z"axis shows the normalized frequency $\omega a/2\pi c = a/\lambda$ where "ω" is the angular frequency, "a" is the lattice period, "c" is the speed of light in vacuum, and "λ" is the free space wavelength. The first PBG exists over the normalized frequency range of $0.2958a/\lambda$ to $0.4359a/\lambda$ for TE mode and the wavelength range is 1239nm to 1826nm.

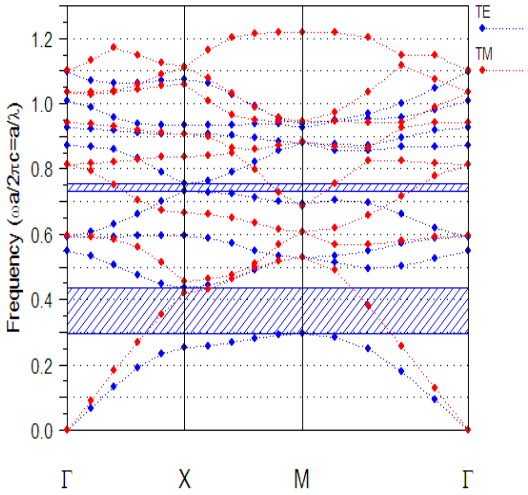

Fig. 2. Band diagram before introducing defect

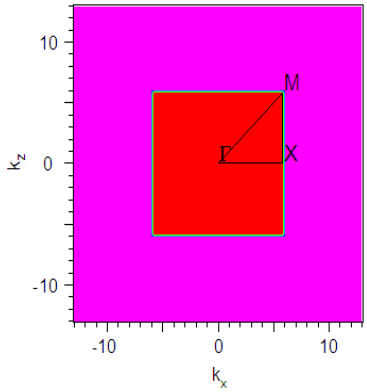

Fig. 3. Brillouin zone and K-Path for the structure

Unique structures are proposed for 1×2, 1×3, 1×4 and 1×6 power splitters. All the four designs are tuned in the same way so as to obtain considerable results. Except 1×2 splitter, the other three structures have a common diamond shaped structure of rods at the junction area of the splitting region. The radii of rods at the splitting region are set as 0.05μm while the radii of rods in the input and output lines of the splitter are about 0.075μm for all the four power splitter structures. The transmission efficiency is calculated for all the splitters using 2D FDTD method and the wavelengths at which maximum efficiency is attained are also observed for each structure.

3. Power splitter

3.1. 1 x 2 Power splitter

The schematic structure of 1×2 splitter is depicted in Fig. 4. The splitter has a Y-junction bend and to obtain almost equal splitting at the two output ports, bi-periodicity is introduced by inserting rods at the splitting region. Here, periodicity is incorporated by inserting a rod with same radius with half lattice constant. The 3D view of the splitter is illustrated in Fig. 5 from which the size of the structure is observed to be 11.4μm×11.4μm.

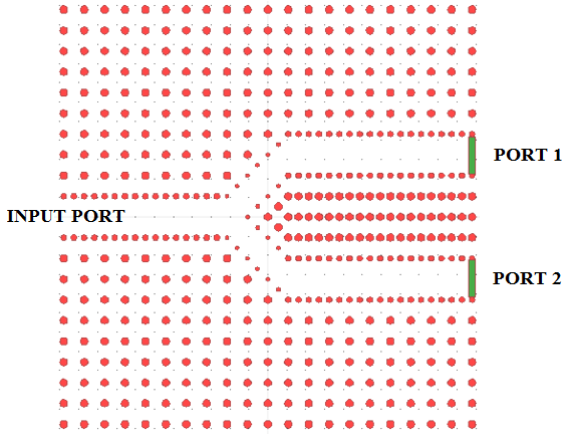

Fig. 4. Schematic structure of 1×2 power splitter

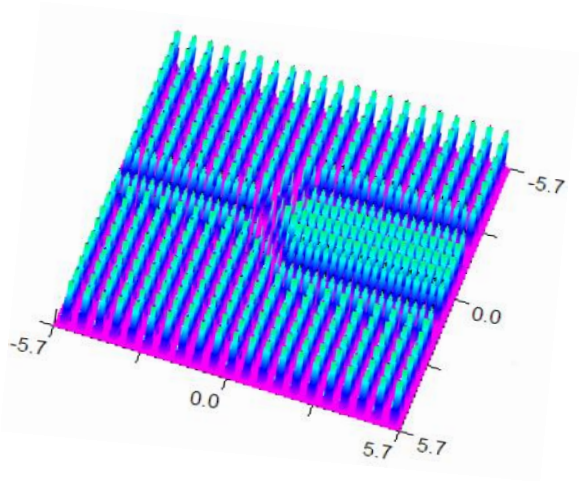

Fig. 5. 3D view of 1×2 splitter

Ideally, input power is equally divided into the output ports without any significant reflection and radiation loss. The operating wavelength range of the proposed 1×2 power splitter is 1510nm to 1535nm. The transmission efficiency of this power splitter is 100% as shown in Fig. 6.

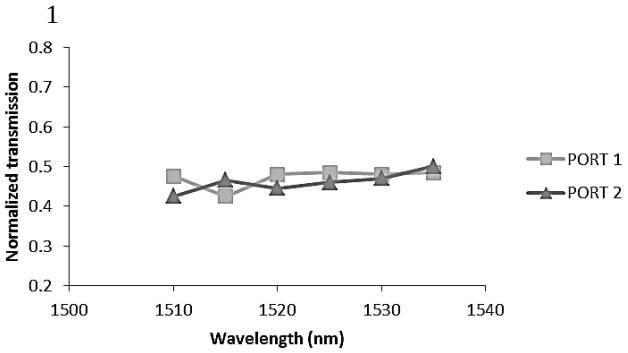

Fig. 6. Normalized transmission spectrum of 1×2 power splitter

In the conventional design, the Y splitter is designed and its functional parameters are accounted. However, the output power is reduced at resonance due to the leakage of the power in the waveguide which reduces the output

transmission. In order to minimize the leakage power at resonance, the biperiodicity in the waveguide is incorporated which reduces the power leakage and increases the output power. The biperiodicity is introduced by inserting a new rod between the existing rods with same or different rod radius.

3.2. 1×3 Power splitter

The structure of 1×3 power splitter is depicted in Fig. 7. The splitter has a Y-junction bend and to obtain almost equal splitting at the three output ports, biperiodicity is introduced by inserting rods at the splitting region. A diamond shaped structure of rods is created at the center of the splitting region. In 1×3 splitter, there are three size of rod radius is used in this structure i.e. r1, r2, r3.The value of r1, r2 and r3 are 0.05μm, 0.0.75μm and0.1μm, respectively. The radius of r1 r2 and r3 is optimized to get better efficiency. The three different radius rods is introduced in this design, which reduces the scattering loss and to improve the output efficiency in the operating wavelength.

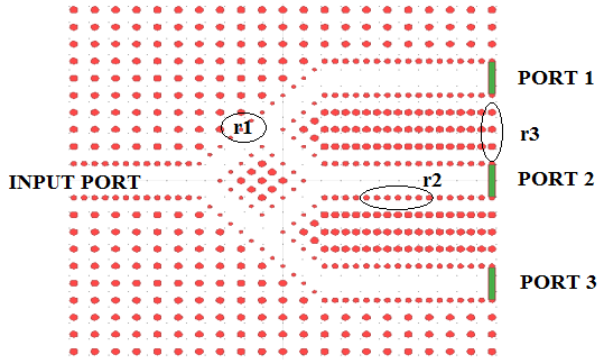

Fig. 7. Schematic structure of 1×3 splitter

The transmission spectrum for the 1×3 splitter is shown in Fig. 8. which implies that the maximum efficiency is 95%. The operating wavelength range of the proposed 1×3 power splitter is 1465nm to 1495nm.

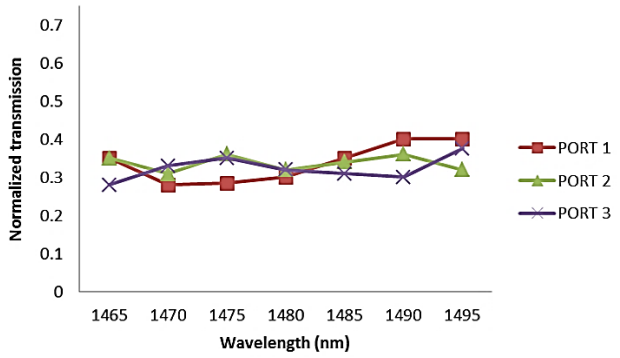

Fig. 8. Transmission spectrum of 1×3 splitter

3.3. 1×4 Power splitter

The design of 1×4 splitter is depicted in Fig. 9. The number of rods in the 'X' and 'Z' directions are 35×27. The splitter has a V shaped Y-junction bend and to obtain almost equal splitting at the four output ports, bi-periodicity is introduced by inserting rods at the splitting region. A diamond shaped structure of rods is created at the center of the splitting region which is lined up to the outer line of rods.

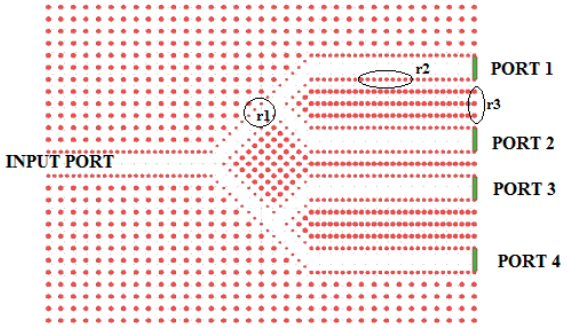

Fig. 9. Schematic structure of 1×4 power splitter

Basically the whole structure is divided into two stages. First stage consists of one Y junction and second stage consists of two Y-junctions. The two stages cascade each other. The configurations of holes size of 2nd and 3rd Y-junction are similar as 1st Y junction. A continuous optical pulse is injected into the first Y-junction and then after propagation of the certain distance these pulses are divided into two channels and coupled into the next stage i.e. 2nd and 3rd Y junction. In the second stage the signal is divided into four channels and achieved the four different power level outputs from the wavelength ranges 1440nm to 1480nm. The output spectrum for the 1×4 splitter is shown Fig. 10 which implies that the maximum efficiency is 97.5% at 1490nm. The operating wavelength range of the proposed 1×4 power splitter is 1440nm to 1480nm.

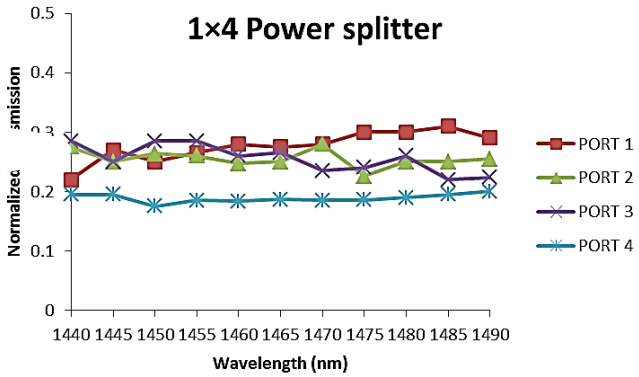

Fig. 10. Normalized spectrum of 1×4 splitter

3.4. 1×6 Power splitter

The structural design of 1×6 splitter is shown in Fig. 11. The total number of rods in the 'X' and 'Z' directions are 35 and 35, respectively. The splitter has a Y-

junction bend and to obtain almost equal splitting at the six output ports, bi-periodicity is introduced by inserting rods at the splitting region.

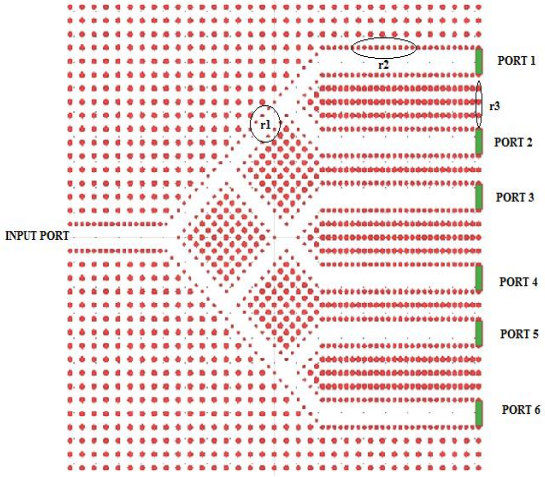

Fig. 11. Structural design of 1×6 power splitter

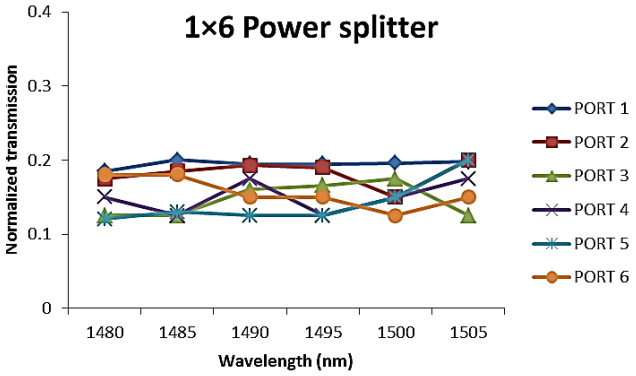

Fig. 12. Transmission spectrum for 1×6 splitter

The normalized transmission spectrum for the 1×6 power splitter is shown in Fig. 12. which implies that the maximum efficiency is 95%. The operating wavelength range of the proposed 1×3 power splitter is 1480nm to 1505nm.

4. Field distributions of power splitter

The Gaussian input signal is launched into the input ports. The normalized transmission spectra are obtained at the output ports by conducting Fast Fourier Transform (FFT) of the fields which are calculated by the 2D FDTD method. The input and output power monitors are positioned at the input and output ports as shown in Fig. 13. The electric field distribution of proposed 1×2, 1×3, 1×4 and 1×6 power splitters are shown in Fig. 13, Fig.14, Fig. 15 and Fig.16, respectively. It is also noticed that the transmission efficiency of the proposed power its reduced while increasing the number of splitting region. The power reduction is due to scattering when the numbers of ports are increased.

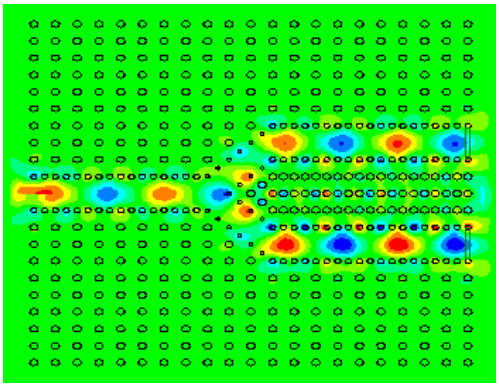

Fig. 13. Field distributions for 1×2 power splitters

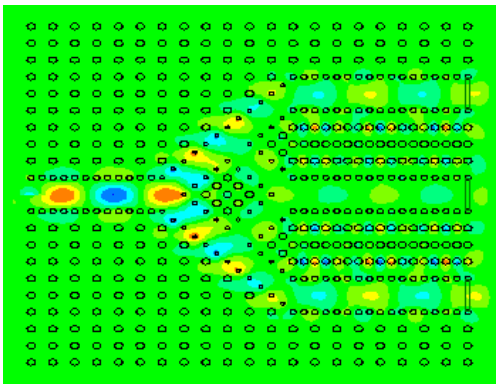

Fig. 14. Field distributions for 1×3 power splitters

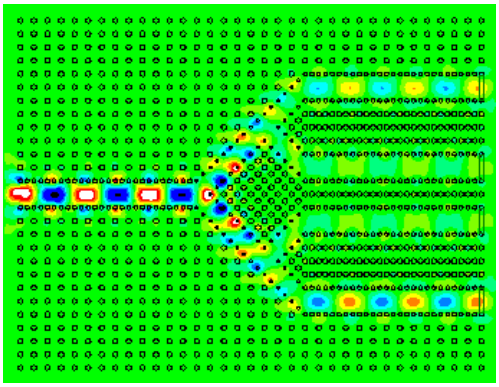

Fig. 15. Field distributions for 1×4 power splitters

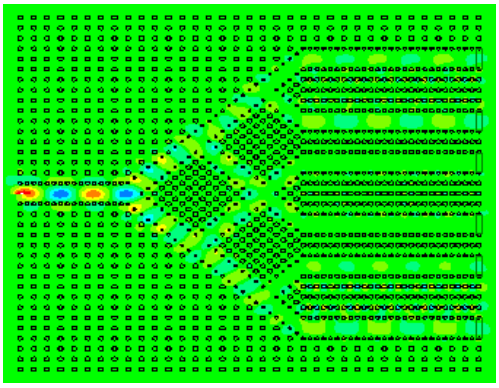

Fig. 16. Field distributions for 1×6 power splitters

Table.1. Comparison of operating wavelength, transmission efficiency and it's size of the proposed 1×2, 1×3, 1×4 and 1×6 power splitters

Design	Size	Operating Wavelength (nm) range	Transmission Efficiency (%)
1×2	11.4μm× 11.4 μm	1510 to 1535	100
1×3	11.4 μm× 11.4 μm	1465 to 1495	95
1×4	19 μm× 14.6 μm	1440 to 1480	97.5
1×6	19 μm× 19 μm	1480 to 1505	95

The input signal is coupled perfectly into the output port during its operating wavelength range. Alternatively, the power either reflected back to the source or partially coupled at other wavelength ranges.

The comparison of the simulation results of the proposed four splitters are listed in the Table 1. From the table, it is noticed that maximum transmission efficiency of the power splitter is about nearly 100% at the operating wavelength and the size is also very miniature. Hence the proposed device could be implemented for integrated optics.

The functional parameters of the proposed power splitter are compared with the reported one which are listed in Table 2. From the table it is observed that the power splitters are primarily designed using square and hexagonal lattice with 1*2, 1*3, 1*4 ports. Almost all the power splitters are designed to operate at 1550nm using Y junction and T junction. If the transmission efficiency of the splitter is high, either the size is larger or bandwidth is smaller. If the bandwidth wider, the transmission efficiency is lower. In this attempt, the proposed power splitter provides high transmission efficiency, wider bandwidth with lower size.

The fabrication step of proposed and designed PC based power splitter is discussed here. The PC based power splitter square lattice is realized through SOI wafer. The SOI wafer is fabricated with stack material of Si-Sio_2-Si whose respective thickness are 200 nm-1000 nm-450 nm, respectively.

Table 2. Functional parameters comparision of proposed power splitter with existing power splitter

Authors/Year	**Lattice Structure**	**Structure Type**	**No of Ports**	**Size**	**Operating wavelength range**	**Transmission Efficiency**
Tianbou Yu et al. 2011 [44]	Square	Y Splitter	1*3	10*12μm^2	1500nm – 1590nm	80.6%-99.5%
Md. Mahfuzur Rahuman et al. 2012 [45]	Square	Y Splitter	1*2	21*15μm^2	1300nm – 1550nm	--
Rajib Ahmed et al. 2013 [46]	Hexagonal	T Splitter	1*4	10*8μm^2	1500nm	92.8%
Hong Wang et al. 2015 [41]	Hexagonal	Y Splitter	1*4	12*12 μm^2	1493nm -1574nm	99.4%
Sowmiya et al. 2017 [47]	Square	Y Splitter	1*2	--	1550 nm	55.4%
Hadi Razmi et al. 2017 [48]	Hexagonal	Y Splitter	1*2	--	1560nm	90%
Mohammad Danaie et al. 2018 [49]	Hexagonal	Y Splitter	1*2	--	1550nm	98%
Jindal et al. 2018 [50]	Hexagonal	Y Splitter	1*2	21*15μm^2	1900nm	60%
Bani Gandhi et al. 2018 [51]	Hexagonal	T Splitter	1*4	21*15μm^2	1500nm	80%
In this work	**Square**	**Y Splitter**	**1*2**	**11.4*11.4 μm^2**	**1510 nm-1535nm**	**100%**
			1×3	**11.4*11.4 μm^2**	**1465 nm- 1495nm**	**95**
			1×4	**19 *14.6 μm^2**	**1440 nm -1480 nm**	**97.5**
			1×6	**19*19 μm^2**	**1480 nm – 1505 nm**	**95**

Once SOI is formed, then 100 nm thick of polymethylmethacrylate (PMMA) resist material is spin coated over SOI wafer at 7000 rpm for 15 minutes. The PMMA is utilized for making a mask pattern in the SOI substrate. This mask pattern is designed using *CleWin* 4.1-layout editor. Before going to the lithography process, the PMMA resist is moving through a soft bake with the temperature of 110^{o}C for 10 minutes. Once the process is completed, then the wafer is ready for lithography. During fabrication several techniques used for lithography like optical lithography, Electon Beam lithography and Focused Ion beam lithography is reported already. In the proposed design, E-Beam Lithography is needed for the proposed design due to accurate vertical etching for few tens of nanometers. The other techniques do not have capability to control the feature size in sub nm size Particularly, Raith E line direct electron beam lithography is needed as it provides ultra-high resolution, maximum acceleration voltage of up to 30kV and nano manipulators to get the pattern of the air hole structure. Then, the developed substrate is hot baked with 180^{o} C for dehydration process.

The Deep Reactive Ion Etching (DRIE) is the deep vertical dry etching which is used to form the array of holes based on the masking pattern. Next wet etching process is used to remove the Sio_2 oxide layer rinse with BHF acid for 16 minutes. The Sio_2 oxide layer is acting as sacrificial layer for suspending the PC in air. By having the aforementioned fabrication steps, the proposed power splitter will be realized.

5. Conclusion

The two-dimensional PC square lattice based 1×2, 1×3, 1×4 and 1×6 power splitters are designed and investigated through FDTD method. The wavelengths at which the maximum efficiency is achieved in the wavelength range of 1510nm to 1535nm, 1465nm to 1495nm, 1440nm to 1480nm, 1480nm to 1505nm for 1×2, 1×3, 1×4 and 1×6 splitters respectively. The input power is observed to split almost equally into the output ports with the transmission efficiency about and more than 95% for all the structures. The sizes of the splitters are found to be compact and hence the proposed devices are suitable for application in the optical communication systems.

References

[1] John D. Joannopoulos, Joshua N. Winn, Robert D. Mead, Princeton Press, Princeton, NJ, 1995.

[2] J. D. Joannopoulos, Pierre R. Villeneuve, Shanhui Fan, Nature **386**, 143(1997).

[3] Hongjun Liu, Nan Huang, Qibing Sun, Yangang Lu, Zhaolu Wang, Journal of Modern Optics **63**(3), 224 (2016).

[4] Dongxia Zhuang, Guimin Lin, Xiyao Chen, Optik, **125**(16), 4322 (2014).

[5] Farhad Mehdizadeh, Mohammed Soroosh, Photon Network Communications **31**(5), 65(2016).

[6] Fei Fan, Jining Li, Sheng-Jiang Chang, Xiang-Hui Wang, Yan Liu, Optics Communications **336**(25), 59 (2015).

[7] Changqing Guo, Fangfang Wu, Jie Zhou, Lulu Li, Yifeng Shen, Yongchun Wang, Yuan Zhang, Optics Communications, **285**(35), 2846 (2012).

[8] Ashkan Pashamehr, Hamed Alipour-Banaei, Mahdi Zawari, Frontiers of Optoelectronics **13**(5), 1 (2016).

[9] Farhad Mehdizadeh, Hamed Alipour-Banaei, Mohammad Soroosh, Optical and Quantum Electronics **48**(28), 1 (2016).

[10] Deyan Chen, Jing Qiao, Juebin Wang, Shangbin Tao, Yali Duan, Photonic Sensors **6**(2), 137 (2016).

[11] Masahiro Tanaka, Richard W. Ziolkowski, Optical and Quantum Electronics **31**(1), 843 (1999).

[12] Alejandro Martinez, Amadeu Griol, David Mira, Francisco Cuesta, Jaime Garcia, Javier Marti, Pablo Sanchis and Roberto Llorente, Applied Physics Letters **83**(15), 3033 (2003).

[13] K. B. Chung, J. S. Yoon, Optical and Quantum Electronics **35** (3), 959 (2003).

[14] Hidekazu Sasaki, Kiyoshi Asakawa, Koji Ishida, Kuon Inoue, Naoki Ikeda, Yoshimasa Sugimoto, Yu Tanaka, Japanese Journal of Applied Physics, **43**(4), 446 (2004).

[15] Beom-Hoan O, El-Hang Lee, Hyun-Jun Kim, Hyun-Shik Lee, Insu Park, Kyung-Mi Moon, Se-Geun Park, Seung-Gol Lee, Optics Express **12**(15), 3599 (2004).

[16] Armis R. Zakharian, Jerome V. Moloney, Mahmoud Fallahi, Masud Mansuripur, Tao Liu, Journal of Lightwave Technology **22**(12), 2842 (2004).

[17] Ikmo Park, H. Lim, Sangin Kim, Nanophotonics for Communication: Materials and Devices, SPIE **5597**(15), 129 (2004).

[18] Hanjo Lim, Ikmo Park and Sangin Kim, Optics Letters **30**(3), 257 (2005).

[19] Dongsheng Wang, Junfeng Shi, Shengye Huang, Wei Li, Optical Engineering **45**(2), 1 (2006).

[20] Chun Jiang, Hongliang Ren, Jingyuan Wang, Mingyi Gao, Weisheng Hu, Optical and Quantum Electronics **38**(8), 645 (2006).

[21] Jian-Yi Yang, Ming-Hua Wang, Qing-Hua Liao, Tian-Bao Yu, Xiao-Qing Jiang, Journal of Optics A: Pure and Applied Optics, IOPScience **9**(1), 37 (2007).

[22] M. S. Abrishamian, M. Djavid, A. Ghaffari, F. Monifi, Journal of Applied Sciences **8**(8), 1416 (2008).

[23] M. S. Abrishamian, M. Djavid, A. Ghaffari, F. Monifi, Optics Communications **281**(17), 5929 (2008).

[24] M. S. Abrishamian, M. Djavid, A. Ghaffari, F. Monifi, Journal of Optics A: Pure and Applied Optics, IOPScience **10**(7), 1 (2008).
[25] Afshin Ghaffari, Faraz Monifi, Mehrdad Djavid, Mohammad Sadegh Abrishamian, Journal of Optical Society of America B, OSA Publishing **25**(8), 1231 (2008).
[26] M. S. Abrishamian, Afshin Ghaffari, Faraz Monifi, Mehrdad Djavid, Journal of Optical Society of America B, OSA Publishing **25**(11), 1805 (2008).
[27] M. S. Abrishamian, M. Djavid, A. Ghaffari, Physica E **41**(3), 1495 (2009).
[28] Kazuhiko Ogusu, Zetao Ma, Optics Communications **282**(17), 3473 (2009).
[29] Da Mu, Jianhong Zhou, Jinhua Yang, Lu Wang, Qing Chang, Wenbo Han, Journal of Optical Society of America B, OSA Publishing **26**(12), 2469 (2009).
[30] Afshin Ghaffari, Mehrdad Djavid, Mohammad Sadegh Abrishamian, Applied Optics, **48**(8), 1606 (2009).
[31] Jian Yi Yang, Jun Zhang, Qi Jie Wang, Siu Fung Yu, Tian Bao Yu, Photonics Technology Letters **23**(16), 1151 (2011).
[32] Liguang Fang, Lingjuan He, Nianhua Liu, Tianbao Yu, Xinhua Deng, Optical Engineering **50**(11), 1 (2011).
[33] Fei Fan, Sheng-Jiang Chang, Xiang-Hui Wang, Yu Hou, Optik, **124**(22), 5285, (2012).
[34] Daquan Yang, Huiping Tian, Yuefeng Ji, Optics Communications, Elsevier **285**(18), (2012).
[35] Din Chai Tee, Faisal Rafiq Mahamd Adikan, Nizam Tamchek, Sayed Reza Sandoghchi, Toshio Kambayashi, Journal of Lightwave Technology **30**(17), 2818 (2012).
[36] Alireza Andalib, Hamed Alipour-Banaei, Reza Ghavidel Barsary, Journal of Artificial Intelligence in Electrical Engineering **2**(6), 5 (2013).
[37] Jiu-Sheng Li, Optik **125**(16), 4543 (2014).
[38] F. R. Mahamd Adikan, Y. G. Shee, N. Tamchek, D. C. Tee, Optics Express **22**(20), 24241 (2014).
[39] Hong Wang and Lingjuan He, Optical Engineering **53**(7), 1 (2014).
[40] Foozieh Sohrabi, Seyedeh Mehri Hamidi, Tayebeh Mahinroosta, Optical Engineering **53**(11), 1 (2014).
[41] Hong Wang and Lingjuan He, Modern Physics Letters B, World Scientific **29**(15), 1 (2015).
[42] Jian-Rong Hu and Jiu-Sheng Li, Journal of Infrared Millimeter and Terahertz Waves **64**(2), 1 (2016).
[43] Alireza Tavousi, Mohammad Ali Mansouri-Birjandi, Photonic Network Communications **92**(5), 1 (2016).
[44] Tianbao Yu, Lingjuan He, Xinhua Deng, Liguang Fang, Nianhua Liu, Optical Engineering **50**(11), 114601 (2011).
[45] Md. Mahfuzur Rahman, Mamun Hasan, Saeed Mahmud Ullah, International Journal of Computer applications **60**(14), 0975 (2012).
[46] Rajib Ahmed, Md. Masruf Khan, Rifat Ahmmed, Abdul Ahad, Optics and Photonics Journal **3**, 13 (2013).
[47] M. Sowmiya, Ankita Lothikar, E. G. Anagha, A. Rajesh, IOP conference series: Material Science and Engineering **263**(5), 052042 (2017).
[48] Hadi Razmi, Mohammad Soroosh, Yousef S.Kavian, Journal of Optical Communications **39**(4), 1 (2017).
[49] Mohammad Danaie, Ruhallah Nasiri-Far, Abbar Dideban, International Journal of Optics and Photonics **12**(1), 33 (2018).
[50] P. Jindal, H. J. Kaur, Optoelectronics, Instrumentation and Data processing **54** (6), 574 (2018).
[51] Bani Gandhi, Anil Kumar Shukla, Indian Journal of Science and Technology **12**(7), 1 (2018).

*Corresponding author: arunec002@gmail.com